

Surround-View Vision-based 3D Detection for Autonomous Driving: A Survey

Apoory Singh¹ Varun Bankiti¹

Abstract

Vision-based 3D Detection task is fundamental task for the perception of an autonomous driving system, which has peaked interest amongst many researchers and autonomous driving engineers. However achieving a rather good 3D BEV (Bird’s Eye View) performance is not an easy task using 2D sensor input-data with cameras. In this paper we provide a literature survey for the existing Vision Based 3D detection methods, focused on autonomous driving. We have made detailed analysis of over 60 papers leveraging Vision BEV detections approaches and highlighted different sub-groups for detailed understanding of common trends. Moreover, we have highlighted how the literature and industry trend have moved towards surround-view image based methods and note down thoughts on what special cases this method addresses. In conclusion, we provoke thoughts of 3D Vision techniques for future research based on shortcomings of the current techniques including the direction of collaborative perception. Regularly updated summary can be found at <https://github.com/ApooryRobotacist/VisionBEVDetectionSurvey>.

1. Introduction

Object detection is a trivial task for humans. Pretty much any teenager can look at the scene out the car’s windscreen and place all the agents, dynamic or static, on a mental BEV (Bird’s Eye View) map. This virtual map includes per agent information, but not limited to - center coordinates, dimensions, angle of view, orientation angle etc. However, teaching this to a computer has been an uphill task until the turn of the last decade. This task entails identifying and localizing all instances of an object (like cars, humans, street signs, etc.) within the field of view as shown in Figure 1. Similarly classification,



Figure 1. Surround-view Image 3D Detector in autonomous driving. Ground-truth 3D boxes overlaid over surround-images in perspective view (top); Ground-truth 3D boxes overlaid over BEV HD Map (bottom), with ego car in pink.

segmentation, dense-depth estimation, motion prediction, scene understanding etc, have been the other fundamental problems in computer vision.

Early object detection models were build on hand-crafted feature extractors such as Viola-Jones detector (Viola & Jones, 2001), Histogram of Oriented Gradients (HOG) (Dalal & Triggs, 2005) etc. Them being SOTA of their time, however, compared to the current methods these methods are slow, inaccurate and not scalable on generic datasets. Introduction of convolutional neural network (CNNs) and deep learning for image classification changed the landscape of visual perception. CNN’s use in ImageNet Large Scale Visual Recognition Challenge (ILSVRC) 2012 challenge by AlexNet (Krizhevsky et al., 2012) has inspired further research in computer vision industry. Mainstream applications of 3D object detection lies around autonomous driving, mobile -robotic vision, security cameras etc. Camera has a limited Field-of-view (FOV), it has led to the next breakthrough research field of *how to leverage views from multiple cameras to reason the surroundings*.

¹Motional, Pittsburgh, USA. Correspondence to: Apoory Singh <apoory.singh@motional.com>, Varun Bankiti <varun.bankiti@motional.com>.

Contributions from Computer-Vision team at Motional.

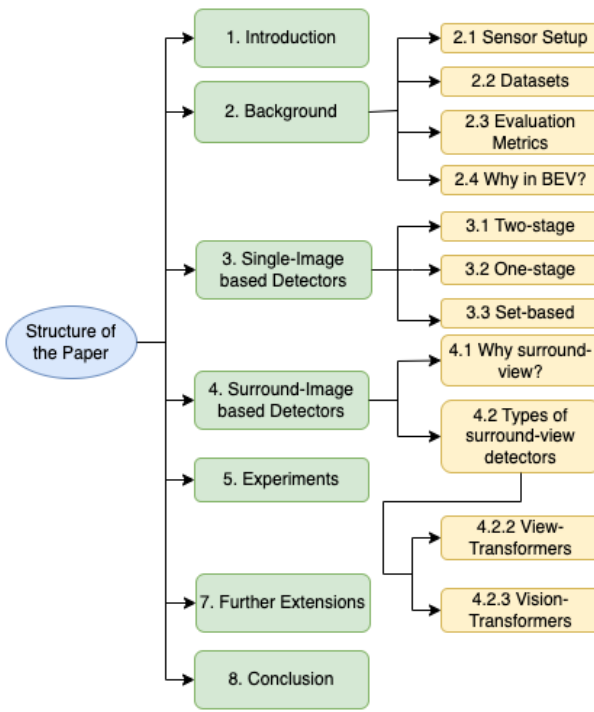


Figure 2. Structure of this Survey Paper.

This survey on Surround-view Vision-based 3D object detection provides a comprehensive review of deep learning based methods and architectures in the recent past. The main contributions of this paper are as follows:

- This paper provides an in-depth analysis of major single-view detector baselines that inspired surround-view detector research in 3D object detection task using cameras.
- This paper provides further analysis of major surround-view detector trends currently in-development in the computer-vision industry; thereby categorizing them to follow-through easily.
- This paper provided detailed background on evaluation metrics and datasets used to evaluate and compare above methods.
- It makes detailed analysis about the remaining problems and introduce several potential research directions about the BEV 3D image object detectors, hence opening the door for future research.

Rest of the paper is organized as follows: We first look at the background information required to understand autonomous driving 3D detections viz., evaluation metrics, datasets, annotations etc. in Section 2. Then, we introduce single-image

based detection methods and top SOTA approaches that inspired surround-view approaches in Section 3. In Section 4, we dive into details for surround-image based detections approaches focused on autonomous driving. We then report and analyse performance of these approaches on our previously defined metrics in Section 5. Then in Section 6, we report possible research extensions on surround-view object detection methods that may enlighten future research. Finally in Section 7, we concluded the paper.

2. Background

In order to cover the basics required to understand 3D BEV object detection tasks, we discuss four aspects: Sensor setup on an autonomous vehicle (AV); frequently used datasets; common evaluation metrics for detection task in autonomous driving, and Why Bird's Eye View (BEV) is important for an AV camera perception?

2.1. Sensor Setup

Before we even look at how cameras are setup in an autonomous vehicle (AV), lets try to understand why we need cameras at the first place. Cameras have the most densely packed information compared to other sensors, making them one of the most challenging, sensors to extract information from in an AV, however the most useful at the same time. To understand this mathematically let us look at the number of data points in each of the visualizations as in Figure 3. Take these data points (floating point numbers) are the input to the perception algorithm for a sensor to cover a 360° view, that is responsible to make decisions for an AV.

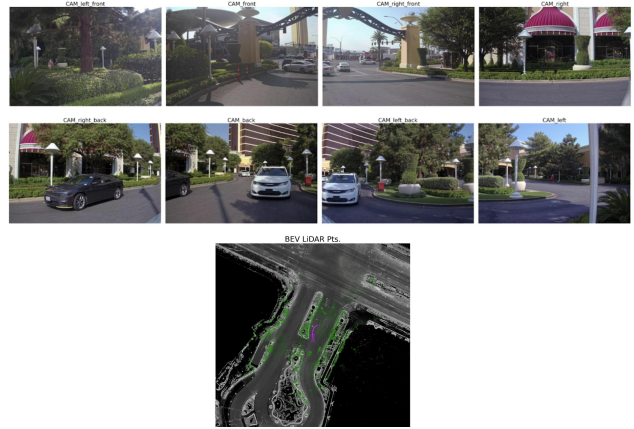


Figure 3. Surround-view 8 camera images (top); LiDAR Point Cloud overlaid over an HD Map (bottom). Key: Green points: LiDAR point cloud; Pink box: Autonomous vehicle; Gray map: Pre-computed HD map with color intensity.

Let's start with the camera:

Number of cameras: 8;

Number of pixels per camera: $2,000 * 3,000$ (image pixel resolution: width*height);

Representation of a pixel: 3 (three channeled RGB value).

*This brings total parameters to: $8 * 2000 * 3000 * 3 = 144M$ float numbers!*

Similar comparison with a LiDAR now:

Number of LiDAR points in a point cloud: 250,000;

Representation of each LiDAR point: 4 (3D coordinate (x, y, z) and reflectance).

*This brings total parameters to: $250,000 * 4 = 1M$ float numbers!*

These numbers and visualizations as in Figure 3 should be enough to prove our point of “*the key role cameras play in an AV perception to perceive the environment.*”

A camera is one of the least expensive sensor too compared to other laser based as well. However, they are spectacularly better for detecting long-range objects; and extracting vision-based road cues like state of traffic lights, stop signs etc, compared to any other laser sensors. There's a setup of surround-cameras on an AV, which may vary depending on different autonomous car companies. Typically there are $6 \sim 12$ cameras per vehicle. These many cameras are needed to cover the entire surrounding 3D scene. We are limited to use cameras with normal FOV (Field of view) otherwise we may get image distortions that are beyond recovery, like with Fish-eye cameras (Wide FOV), which are only good for up to few tens of meters. A perception sensor setup in one of the most cited benchmark-dataset, nuScenes (Caesar et al., 2020) in the AV space can be seen in Figure 4.

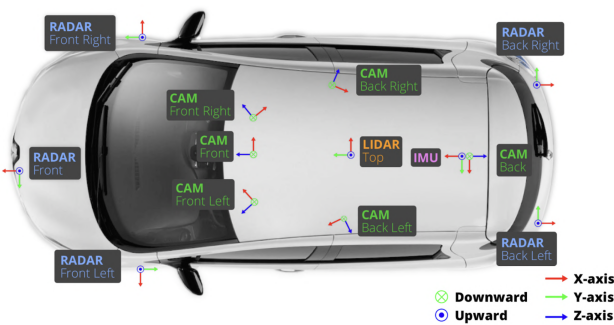


Figure 4. Sensor setup for an Autonomous vehicle in nuScenes benchmark dataset.

2.2. Datasets

nuScenes(Caesar et al., 2020), KITTI(Geiger et al., 2012), Waymo Open Dataset (WOD)(Sun et al., 2020) are the three

most commonly used datasets for 3D BEV object detection task. Apart from them, H3D(Patil et al., 2019), Lyft L5(Houston et al., 2020) and Argoverse(Chang et al., 2019) can also be used for BEV perception tasks. nuScenes contains 1000 scenes with a duration of 20 seconds each. They contain six calibrated images covering the 360° view of the road. Sensor setup with nuScenes can be seen in Figure 4. KITTI was the seminal work on autonomous driving dataset. It consists of a smaller sample of data compared to the more recent ones. Waymo Open Dataset (WOD) is another large-scale autonomous driving dataset with 798 sequences training, 202 validation and 150 testing sequences respectively. Argoverse 2 also contains 1000 scenes with LiDARs, stereo imagery and ring camera imagery, also known as surround-view camera systems. Detailed information of these dataset is given as in Table 1.

2.3. Evaluation Metrics

3D object detectors use multiple criteria to measure performance of the detectors viz., precision and recall. However, mean Average Precision (mAP) is the most common evaluation metric. Intersection over Union (IoU) is the ratio of the area of overlap and area of the union between the predicted box and ground-truth box. An IoU threshold value (generally 0.5) is used to judge if a prediction box matches with any particular ground-truth box. If IoU is greater than the threshold, then that prediction is treated as a True Positive (TP) else it is a False Positive (FP). A ground-truth object which fails to detect with any prediction box, is treated as a False Negative (FN). Precision is the fraction of relevant instances among the retrieved instances; while recall is the fraction of relevant instances that were retrieved.

$$\text{Precision} = \text{TP}/(\text{TP} + \text{FP}) \quad (1)$$

$$\text{Recall} = \text{TP}/(\text{TP} + \text{FN}) \quad (2)$$

Based on the above equations, average precision is computed separately for each class. To compare performance between different detectors (mAP) is used. It is a weighted mean based on the number of ground-truths per class.

In addition, there are a few dataset specific metrics viz., KITTI introduces Average Orientation Similarity (AOS), which evaluates the quality of orientation estimation of boxes on the ground plane. mAP metric only considers 3D position of the objects, however, ignores the effects of both dimension and orientation. In relation to that, nuScenes introduces TP metrics viz., Average Translation Error (ATE), Average Scale Error (ASE) and Average Orientation Error (AOE). WOD introduces Average Precision weighted by Heading (APH) as its main metric. It takes heading/ orientation information into the account as well. Also, given depth confusion for 2D-sensors like

Table 1. Information on benchmark dataset commonly used for 3D BEV Object Detection using cameras in autonomous driving.

DATASET	CAMERAS	SCENES	TRAIN	TEST	BOXES	CLASSES	TEMPORAL	LiDAR	RADAR
NUSCENES	6	1,000	28,130	6,008	1.4M	10	✓	✓	✓
KITTI (3D)	-	-	7,418	7,518	200K	3	✓	✓	✗
WOD	5	1,150	122,200	40,077	12M	4	✓	✓	✗
ARGOVERSE	7	113	39,384	12,507	993K	15	✓	✓	✗
LYFT L5	6	366	22,690	27,468	1.3M	9	✓	✓	✗
H3D	3	160	8,873	13,678	1.1M	8	✓	✓	✗

camera, WOD introduces Longitudinal Error Tolerant 3D Average Precision(LET-3D-AP), which emphasizes more on lateral errors than longitudinal errors in predictions.

2.4. Why BEV?

There are number of reasons why using 3D agent's representation in a Bird's Eye View makes practical sense for autonomous driving:

- It makes fusion with other 360° sensors i.e. LiDARs and RADARs are more natural as later operate in 360° BEV natively.
- If we operate in BEV, we can model temporal consistency of the dynamic scene much better. Motion compensation i.e. translation and rotation modeling in BEV agents is much more trivial compared to the perspective-view (camera-view). For example; In BEV view: Pose change depends just on the motion of the agent, whereas in perspective-view, pose change depends on the depth as well as the motion of the agent.
- Scale of the objects are consistent in BEV, but not so much in the perspective view. In perspective view objects appear bigger when they are closer to us. Hence, BEV view makes it easier to learn feature scale consistencies.
- In autonomous driving, downstream tasks after perception, like motion prediction and motion planning operate on the BEV natively. It makes natural sense for all the software stacks to work in a common coordinate-view system on a robotic platform.
- Newly researched field - Collaborative perception which we will talk about in the later section also utilizes BEV representation for representing agents at a common coordinate system, else each agent will have their own perspective view.

3. Single-Image Based Detectors

We have divided single-view image based object detection based on the three categories: two-stage, single-stage and

set-based detectors. However, we would like to mention pioneer works like Viola-Jones ([Viola & Jones, 2001](#)), HOG Detector ([Dalal & Triggs, 2005](#)), Deformable Parts Model (DPM) ([Girshick et al., 2014](#)) which have revolutionized computer vision in PASCAL VOC challenge in 2009 ([Zhang et al., 2007](#)). These approaches uses classical computer-vision techniques which relies on extracting heuristic features.

3.1. Two-stage Detectors

This is a class of detectors, divided into two stages. First stage is to predict arbitrary number of object proposals, and then in second stage they predict boxes by classifying and localizing those object proposals. However, these proposals have inherent problem of slow inference time, lack of global context (even within the single image) and complex architectures. Pioneer work with two-stage approach are: Region-based fully convolution network (R-FCN) ([Dai et al., 2016](#)), Feature Pyramid Network (FPN) ([Lin et al., 2016](#)) and Mask R-CNN ([He et al., 2017](#)) which are built upon R-CNN ([Girshick et al., 2013](#)) line of work. There's also a parallel stream of work around Pseudo-LiDAR ([Wang et al., 2018](#)) in which dense-depth is predicted in the first stage, thereby converting pixels to a pseudo point-cloud and then LiDAR like detection head is applied on the point cloud for 3D object detection as done in Point-pillars ([Lang et al., 2018](#)).

3.2. Single-stage Detectors

YOLO ([Redmon et al., 2015](#)) and SSD ([Liu et al., 2015](#)) opened the gate for single-stage detectors. These detectors classify and localize semantic objects in a single shot using dense-predictions. However, they rely heavily on post-processing Non-maximum Suppression (NMS) step to filter out duplicate predictions, as one of the problem. Their dependence on anchor boxes heuristics was addressed in Fully Convolutional One-Stage Object Detection (FCOS) ([Tian et al., 2019](#)) to predict 2D boxes. Extension of this work is seen in FCOS3D ([Wang et al., 2021a](#)) where they address 3D object detection problem, by regressing 3D

parameters per object. These methods still heavily rely on post-processing for duplicate detections.

3.3. Set-based Detectors

This approach removes hand-designed NMS using set-based global loss that forces unique predictions per object via bipartite matching. The pioneer paper, DETR (Carion et al., 2020) started this chain of work. However it suffers through slow convergence which limited spatial resolution of features. However, it was later addressed in Deformable-DETR (Zhu et al., 2020) method which replaces the original global dense attention with deformable attention that only attends to a small set of sampled features to lower the complexity thereby speeding up the convergence. Another approach to accelerate convergence is SAM-DETR (Zhang et al., 2022) which limits the search-space for attention module by using the most discriminative features for semantic-aligned matching. This line of work still has a CNN based backbone, however they use transformer (Vaswani et al., 2017) based detection head.

Above mentioned approaches operate per-camera, however autonomous driving application needs to address the entire 360° scene which includes 6 ~ 12 surround-cameras covering the entire spatial scene. Per-camera detections are generally aggregated using another set of NMS filtering to get rid of repeat detections originating from the camera overlap Field of View (FOV) regions. AVs need to maintain this long-range FOV overlap to minimize blind-spots in the short range. Perspective view detections are lifted to BEV view either by regressing depth per objects or using heuristic based method, Inverse Perspective Mapping, by estimating ground-plane height.

4. Surround-Image Based Detectors

There are multiple applications of surround-camera based computer-vision (CV) systems like surveillance, sports, education, mobile phones, Autonomous Vehicles. Surround-view systems in sports are making a huge role in the sports analytics industry. It lets us record the right moment across the field at the right moment with the right viewing angle. Surround-view vision has also spread its application in class monitoring systems, which lets teachers give personalized attention to each student in the class. Nowadays it is hard to find any smart phone with a single camera. For these applications, surround-view system enables capturing the right resolution with a good field of view with minimum distortions. However, to limit the scope of this paper we will focus on Autonomous driving based CV.

A surround-view system makes use of features from different views to understand the holistic representation of the scene around the autonomous vehicle. A combination of any two or more cameras requires prior infrastructure work related to fixed sensor mountings and their calibration. Calibration of the camera simply means extracting the extrinsics transformation matrix between the two cameras. This camera matrix enables us to make one-to-one mapping of a pixel in a camera to a pixel in another camera, hence creating a relation between multiple cameras to enable reasoning between themselves.

Surround-view images can be represented by $\mathbf{I} \in \mathbb{R}^{N \times V \times H \times W \times 3}$. Here, N, V, H and W are the number of temporal-frames, number views, height and width respectively.

4.1. Why surround-view in an AV?

Lot of times it is hard to fit the entire object in the single frame to accurately detect and classify it. This is a specially common issue with long vehicles. Let's take a visual understanding of what this means in as Figure 5

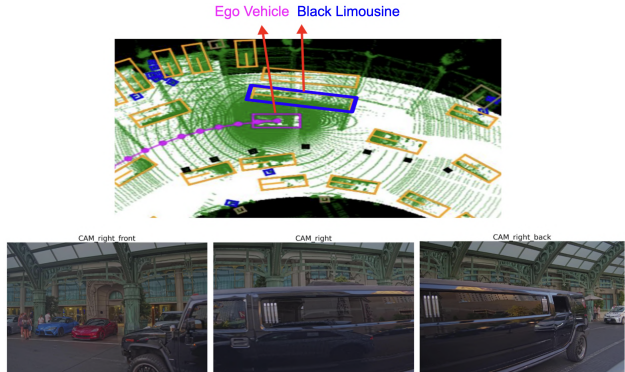


Figure 5. Usage of surround-view images in 3D object detection problem. BEV view (top); surround-view images of right-front, right, right-back cameras (bottom). This shows that with one or two of the cameras we may classify object as car, but without all the three images we won't be able to perfectly localize i.e. fit a bounding box on the black limousine.

4.2. Types of Surround-view Detectors

SOTA surround-view Detections can be broadly classified amongst two subgroups - Geometry based view transformers and Cross-attention based vision-transformers (ViT).

4.2.1. VIEW TRANSFORMERS

Pioneer work Lift, Splat, Shoot (Phlion & Fidler, 2020) started a chain work where they *lift* each image individually into a frustum of features, then *splat* all frustums onto a

rasterized BEV grid. Given n images $\mathbf{X}_k \in \mathbb{R}^{3 \times H \times W}_n$, each with an extrinsics matrix $\mathbf{E}_k \in \mathbb{R}^{3 \times 4}$ and an intrinsics matrix $\mathbf{I}_k \in \mathbb{R}^{3 \times 3}$, we can find a rasterized BEV map of the feature in BEV coordinate frame as $\mathbf{y} \in \mathbb{R}^{C \times X \times Y}$, where C , X , and Y are channel depth, and height and width of BEV map. The extrinsic and intrinsic matrices together define the mapping from reference coordinates (x, y, z) to local pixel coordinates (h, w, d) for each of the n cameras. This approach does not require access to any depth sensor during training or testing, just 3D box annotations are enough. This architecture is demonstrated in Figure 6. One of the latest development on this line of work is BEVDet (Huang et al., 2021), which improves on pre-processing and post-processing techniques.

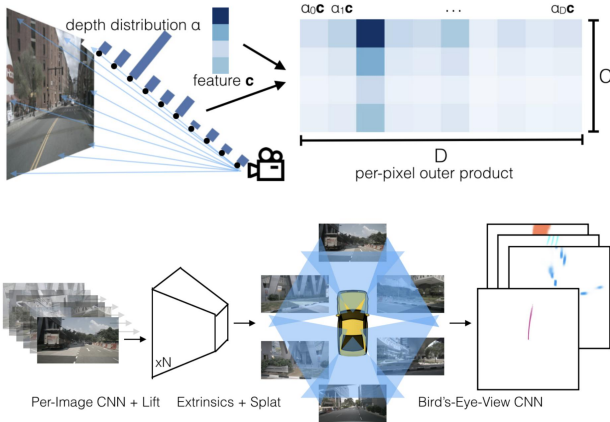


Figure 6. Lift-splat-shoot (LSS) (Phlion & Fidler, 2020) architecture: Lift step is visualized where per-image-frustum's pixel is projected to a discrete depth in BEV coordinate space with a context vector (top). Overall architecture is shown which takes in n images and returns BEV semantic map (bottom).

BEVDet4D (Huang & Huang, 2022a) adds temporal dimensionality to this method and makes it a 4-dimensional problem. They tried to address inherent problem of high velocity error in vision-based detectors. Single-frame vision-based detectors generally have higher velocity errors compared to laser-based sensors as LiDAR detectors generally use multiple-sweep data with temporal information embedded in the point cloud; and RADAR's inherent point cloud includes velocity attribute using Doppler effect. Adding temporal frames in vision-detector enables us to learn temporal cues of the dynamic agent on the road.

As a further extension, BEVDepth (Li et al., 2022b) method adds camera-aware depth estimation module which facilitates the object depth predicting capability. They prove that *enhancing depth is the key to high-performance camera 3D detections* on nuScenes benchmark. They

have replaced vanilla segmentation head in LSS with the CenterPoint (Yin et al., 2020) head for 3D detection. For the auxiliary depth head baseline they use supervision from the detection loss only. However, due to the difficulty of monocular depth estimation, a sole detection loss is far from enough to supervise the depth module. Then used calibrated LiDAR data to project point cloud on to the images using camera transformation matrices hence forming a 2.5D image coordinates $P^{img}i(u, v, d)$, where u and v denote coordinates in pixel coordinate and d denotes depth from the corresponding LiDAR point-cloud. To reduce memory usage, further development of M^2BEV (Xie et al., 2022) decreases the learnable parameters and achieves high efficiency on both inference speed and memory usage.

These detectors include four components: 1. An image encoder to extract the image features, 2. A depth module to generate depth and context, then outer product them to get point features, 3. A view transformer to convert the feature from camera view to the BEV view, and 4. A 3D detection head to propose the final 3D bounding boxes. BEVStereo (Li et al., 2022a) introduces dynamic temporal stereo method to enhance depth prediction within compute cost-budget. Simple-BEV (Harley et al., 2022) introduces RADAR point cloud on LSS approach. Based out of view transformers, BEVPoolv2 (Huang & Huang, 2022b) is the current SOTA as per nuScenes vision-detection leaderboard. They use BEVDet4D based backbone with dense-depth and temporal information for training. They have shown TensorRT runtimes speedups as well, TensorRT is the model format generally used by Nvidia deployment hardwares.

4.2.2. VISION TRANSFORMERS

ViT (Vision Transofmers) can be divided as per the granularity of queries (object proposals) in the transformer decoder as per (Ma et al., 2022) viz., sparse query-based and dense query-based methods. We will go into details about the representative work for both of these categories.

Sparse Query-based ViT: In this line of work, we try to learn object proposals to look for in the scene, from the representative training data, and then use those learned object proposals to query at the test-time. Here assumption is made that test data objects are representative of the training data ones.

Seminal paper, in single-image (Perspective-view), DETR (Carion et al., 2020) started this line of work, which is later extended to surround-view images in BEV with DETR3D (Wang et al., 2021b). Here given n surround-view images $\mathbf{I} \in \mathbb{R}^{H' \times W' \times 3}$, the backbone and/or FPN and/or Transformers encoder produce n encoded image features $\mathbf{F} \in \mathbb{R}^{H' \times W' \times d}$, where d is the feature dimension, and H' ,

W' and H, W denote spatial sizes of the image and the features, respectively. Then these n encoded features and a small set of object queries $\mathbf{Q} \in \mathbb{R}^{N \times d}$ are fed into the Transformer decoder to produce detection results. Here N is the number of the object queries, typically $300 \sim 900$. As a meta-data camera transformation matrices is also used as an input. These matrices are required to create 3D reference point mapping onto the 2D coordinate-space and sample respective 2D-features.

In the Transformer decoder, object queries are sequentially processed by a self-attention module, a cross-attention module, and a feed-forward network (FFN), and then finally to a Multi-Layer Perceptron (MLP) to produce 3D BEV detections as an output. For an interpretation: object queries denote potential objects at different locations on the BEV map; the self-attention module performs message passing among different object queries; and in the cross-attention module, object queries first search for the corresponding regions/ views to match, then distill relevant features from the matched regions for the subsequent predictions. Tesla also released their transformer based work as DETR3D around the same time. Also worth noting, transformer-based encoder is an optional add-on here, but the core part of these detectors is that they have transformer-based decoder. Workflow of this approach can be easily understood in as Figure 7

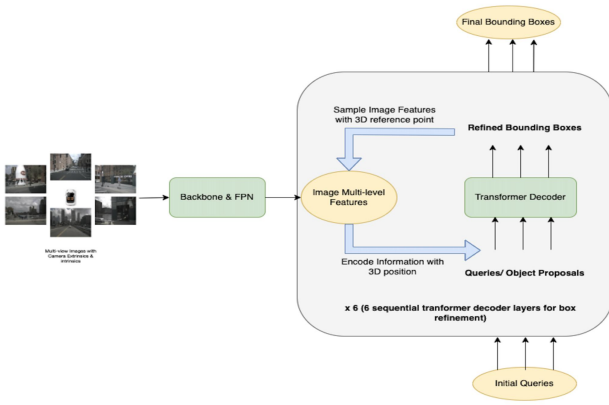


Figure 7. Adaptation workflow from DETR3D (Wang et al., 2021b).

As a further development of this work, Polar DETR (Chen et al., 2022a) parameterizes 3D detections in polar coordinates, which reformulates position parametrization, velocity decomposition, perception range, label assignment and loss function in polar coordinate system (r, θ) . This approach eases optimization and enables center-context feature aggregation to enhance the feature interaction. In Graph-DETR3D (Chen et al., 2022b) they quantify the ob-

jects located at different regions and find that the “truncated instances” (i.e., at the border regions of each image) are the main bottleneck hindering the performance of DETR3D. Although it merges multiple features from two adjacent views in the overlapping regions, DETR3D still suffers from insufficient feature aggregation, thus missing the chance to fully boost the detection performance. To address this issue Graph-DETR3D aggregates surround-view imagery information through graph structure learning (GSL). It constructs a dynamic 3D graph between each object query and 2D feature maps to enhance the object representations, especially at the border regions.

A Positional encoding development work over DETR3D, PETR (Liu et al., 2022a) cites problem with 2D encoding of features in the former approach. They transform surround-view features into 3D domain by encoding the 3D coordinates from camera transformation matrices. Now, object queries can be updated by interacting with the 3D position-aware features and generate 3D predictions, hence making the procedure simpler. A follow-up work PETRv2 (Liu et al., 2022b) adds temporal dimensionality to it to get temporally-aware denser features.

Dense Query-based ViT: Here we have a dense-query based on region of interest in the BEV representation. Each query is pre-allocated with a spatial location in 3D space. This line of work is better than former in the sense that we will still be able to detect certain type of objects that were not learnt as object proposals in the training data with sparse-query. In other words, *this approach is more robust to the scenario when training data is not the perfect representative of the test data.*

Pioneer work with this line of work was BEVFormer (Li et al., 2022c). They exploit both spatial and temporal information by interacting with spatial and temporal space through predefined grid-shaped BEV queries. To aggregate spatial information, they designed spatial cross-attention that each BEV query extracts from spatial features across the camera views. For temporal information, they use temporal self-attention to recurrently fuse the history BEV information as shown in Figure 8. This approach at the time have surpassed sparse-query based ViT’s mentioned above with their higher recall values, exploiting dense queries. However, dense queries come at the cost of compute-budget, which they try to address using deformable-DETR’s (Zhu et al., 2020) K-points around reference point sampling strategy. The fully transformer-based structure of BEVFormer makes its BEV features more versatile than other methods, easily supporting non-uniform and non-regular sampling grids.

A follow-up work BEVFormerv2 (Yang et al., 2022) adds perspective supervision which helps in convergence and

Table 2. Results of vision-only 3D object detections on nuScenes camera-only 3D detection benchmark on test set. Abbreviations defined in Section 5.

METHOD	YEAR	MAP	MATE	MASE	MAOE	MAVE	MAAE	NDS
BEVPOOLV2	2022	0.586	0.375	0.243	0.377	0.174	0.123	0.664
BEVFORMER v2	2022	0.580	0.448	0.262	0.342	0.238	0.128	0.648
BEVSTEREO	2022	0.525	0.431	0.246	0.358	0.357	0.138	0.610
BEVDEPTH	2022	0.503	0.445	0.245	0.378	0.320	0.126	0.600
POLARFORMER	2022	0.493	0.556	0.256	0.364	0.439	0.127	0.572
PETR v2	2022	0.490	0.561	0.243	0.361	0.343	0.120	0.582
BEVFORMER	2022	0.481	0.582	0.256	0.375	0.378	0.126	0.569
BEVDET4D	2022	0.451	0.511	0.241	0.386	0.301	0.121	0.569
GRAPH-DETR3D	2022	0.425	0.621	0.251	0.386	0.790	0.128	0.495
POLARDETR	2022	0.431	0.588	0.253	0.408	0.845	0.129	0.493
BEVDET	2021	0.424	0.524	0.242	0.373	0.950	0.148	0.488
PETR	2022	0.434	0.641	0.248	0.437	0.894	0.143	0.481
DETR3D	2021	0.412	0.641	0.255	0.394	0.845	0.133	0.479
FCOS3D	2021	0.358	0.690	0.249	0.452	1.434	0.124	0.428
CENTERNET	2019	0.338	0.658	0.255	0.629	1.629	0.142	0.400

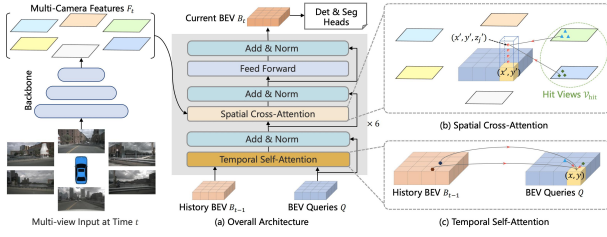


Figure 8. Overall architecture of BEVFormer (Li et al., 2022c). (a) The encoder layer of BEVFormer contains grid-shaped BEV queries, temporal self-attention, and spatial cross-attention. (b) In spatial crossattention, each BEV query only interacts with image features in the regions of interest. (c) In temporal self-attention, each BEV query interacts with two features: the BEV queries at the current timestamp and the BEV features at the previous timestamp.

suits image-based backbone in a better manner. This brings back two-stage detectors, where proposals from the perspective head are fed into the bird's-eye-view head for the final predictions. In addition to the perspective head proposals they also use DETR3D style learned queries. For auxiliary perspective loss, they use FCOS3D (Wang et al., 2021a) head which predicts the center location, size, orientation, and projected center-ness of the 3D bounding boxes. The auxiliary detection loss of this head, denoted as perspective loss L_{pers} , serves as the complement to the BEV loss L_{bev} , facilitating the optimization of the backbone. The whole model is trained with a total objective

$$L_{total} = \lambda_{bev} L_{bev} + \lambda_{pers} L_{pers} \quad (3)$$

PolarFormer (Jiang et al., 2022) reasons that nature of the ego car's perspective, as each onboard camera perceives the

world in shape of wedge intrinsic to the imaging geometry with radical (non-perpendicular) axis. Hence they advocate the exploitation of the Polar coordinate system on top of BEVFormer.

5. Experiments

nuScenes (Caesar et al., 2020) is the widely used datasets in the literature for which sensor setup Figure 4 includes 6 calibrated cameras covering the entire 360° scene. Results on discussed pioneer works are shown on the test set of nuScenes in Table 2. This is under the filter *camera track detections*. The key for the metric abbreviations is as follows: mAP: mean Average Precision; mATE: mean Average Translation Error; mASE: mean Average Scale Error; mAOE: mean Average Orientation Error; mAVE: mean Average Velocity Error; mAAE: mean Average Attribute Error; NDS: nuScenes detection score.

6. Further Extensions

Based on the most-recent developments around the surround-view BEV vision detections, we will now highlight possible future directions for the research.

Deployment compute-budget and run-time constraints: Autonomous vehicle operate on a tight compute budget, as there is a limit of compute resources we can have on-board. However, when 5G internet becomes mainstream and all computation can be transported to the cloud computers. We, industry as a whole should start focusing on run-time constraints of these compute-expensive transformer based networks. One possible direction is to limit the object-proposals (queries) based on input-scene constraints. However, there is a need to have a smart way to handle it,

else these networks may suffer through a low recall issue.

Smart object proposal initialization strategies: We may come with a query initialization strategy that mix-and-match sparse and dense query initialization to enable pros of both. Major con of dense query-based approach is their high run-time. This can be handled by the usage of HD-maps to focus only on the areas of the road which matter the most. Just like BEVFormerV2 (Yang et al., 2022), object proposals can also be take from different modalities. As a one step further, these proposals may also be taken from the past time-step, with a fair assumption that driving scene won't have changed much within a fraction of a second. However, in order to make AVs scalable, researchers need to focus more on affordable sensors like cameras and RADARs and not too much on LiDARs or HD-Maps.

Collaborative Perception: A relatively new field of area is how to make use of multi-agents, mutli-view transformers to enable collaborative perception. This setup requires a minimal infrastructure setup to enable smooth communications between different AVs on the road. CoBEVT (Xu et al., 2022) shows initial proof of how Vehicle-to-Vehicle communication may lead to superior perception performance. They test their performance on OPV2V (Xu et al., 2021) benchmark dataset for V2V perception.

7. Conclusion

In this work we introduced development work around vision-based 3D object detection focused on autonomous vehicles. We went through more than 60 papers and 5 benchmark datasets to prepare this paper.

To be specific, we first build a case on why camera based surround-view detection head is important for solving autonomous vehicles. Then we started off with how research has progressed from single-view detection and extended to surround-view detection head paradigm and thereby increasing the detection performance. We have categorized two prominent categories for surround-view camera detectors to keep an eye on viz., LSS-based and DETR-based. In the end we proposed our take on surround-view detection trends with the focus of deploying those networks on an actual autonomous car, which may enlighten future research work.

References

Caesar, H., Bankiti, V., Lang, A. H., Vora, S., Liong, V. E., Xu, Q., Krishnan, A., Pan, Y., Baldan, G., and Beijbom, O. nuscenes: A multimodal dataset for autonomous driving. In *CVPR*, 2020.

Carion, N., Massa, F., Synnaeve, G., Usunier, N., Kirillov, A., and Zagoruyko, S. End-to-end object detection with transformers. *CoRR*, abs/2005.12872, 2020.

Chang, M.-F., Lambert, J., Sangkloy, P., Singh, J., Bak, S., Hartnett, A., Wang, D., Carr, P., Lucey, S., Ramanan, D., and Hays, J. Argoverse: 3d tracking and forecasting with rich maps. In *Proceedings of the IEEE/CVF Conference on Computer Vision and Pattern Recognition (CVPR)*, June 2019.

Chen, S., Wang, X., Cheng, T., Zhang, Q., Huang, C., and Liu, W. Polar parametrization for vision-based surround-view 3d detection, 2022a. URL <https://arxiv.org/abs/2206.10965>.

Chen, Z., Li, Z., Zhang, S., Fang, L., Jiang, Q., and Zhao, F. Graph-detr3d: Rethinking overlapping regions for multi-view 3d object detection, 2022b. URL <https://arxiv.org/abs/2204.11582>.

Dai, J., Li, Y., He, K., and Sun, J. R-FCN: object detection via region-based fully convolutional networks. *CoRR*, abs/1605.06409, 2016.

Dalal, N. and Triggs, B. Histograms of oriented gradients for human detection. In *2005 IEEE Computer Society Conference on Computer Vision and Pattern Recognition (CVPR'05)*, volume 1, pp. 886–893 vol. 1, 2005. doi: 10.1109/CVPR.2005.177.

Geiger, A., Lenz, P., and Urtasun, R. Are we ready for autonomous driving? the kitti vision benchmark suite. In *2012 IEEE Conference on Computer Vision and Pattern Recognition*, pp. 3354–3361, 2012. doi: 10.1109/CVPR.2012.6248074.

Girshick, R. B., Donahue, J., Darrell, T., and Malik, J. Rich feature hierarchies for accurate object detection and semantic segmentation. *CoRR*, abs/1311.2524, 2013.

Girshick, R. B., Iandola, F. N., Darrell, T., and Malik, J. Deformable part models are convolutional neural networks. *CoRR*, abs/1409.5403, 2014. URL <https://arxiv.org/abs/1409.5403>.

Harley, A. W., Fang, Z., Li, J., Ambrus, R., and Fragkiadaki, K. Simple-bev: What really matters for multi-sensor bev perception?, 2022. URL <https://arxiv.org/abs/2206.07959>.

He, K., Gkioxari, G., Dollár, P., and Girshick, R. B. Mask R-CNN. *CoRR*, abs/1703.06870, 2017.

Houston, J., Zuidhof, G., Bergamini, L., Ye, Y., Chen, L., Jain, A., Omari, S., Iglovikov, V., and Ondruska, P. One thousand and one hours: Self-driving motion prediction dataset, 2020. URL <https://arxiv.org/abs/2006.14480>.

Huang, J. and Huang, G. Bevdet4d: Exploit temporal cues in multi-camera 3d object detection, 2022a. URL <https://arxiv.org/abs/2203.17054>.

Huang, J. and Huang, G. Bevpoolv2: A cutting-edge implementation of bevdet toward deployment, 2022b. URL <https://arxiv.org/abs/2211.17111>.

Huang, J., Huang, G., Zhu, Z., and Du, D. Bevdet: High-performance multi-camera 3d object detection in bird-eye-view. *CoRR*, abs/2112.11790, 2021.

Jiang, Y., Zhang, L., Miao, Z., Zhu, X., Gao, J., Hu, W., and Jiang, Y.-G. Polarformer: Multi-camera 3d object detection with polar transformer, 2022. URL <https://arxiv.org/abs/2206.15398>.

Krizhevsky, A., Sutskever, I., and Hinton, G. E. Imagenet classification with deep convolutional neural networks. In Pereira, F., Burges, C., Bottou, L., and Weinberger, K. (eds.), *Advances in Neural Information Processing Systems*, volume 25. Curran Associates, Inc., 2012. URL <https://proceedings.neurips.cc/paper/2012/file/c399862d3b9d6b76c8436e924a68c45b-Paper.pdf>.

Lang, A. H., Vora, S., Caesar, H., Zhou, L., Yang, J., and Beijbom, O. Pointpillars: Fast encoders for object detection from point clouds, 2018. URL <https://arxiv.org/abs/1812.05784>.

Li, Y., Bao, H., Ge, Z., Yang, J., Sun, J., and Li, Z. Bevstereo: Enhancing depth estimation in multi-view 3d object detection with dynamic temporal stereo, 2022a. URL <https://arxiv.org/abs/2209.10248>.

Li, Y., Ge, Z., Yu, G., Yang, J., Wang, Z., Shi, Y., Sun, J., and Li, Z. Bevdepth: Acquisition of reliable depth for multi-view 3d object detection, 2022b. URL <https://arxiv.org/abs/2206.10092>.

Li, Z., Wang, W., Li, H., Xie, E., Sima, C., Lu, T., Yu, Q., and Dai, J. Bevformer: Learning bird's-eye-view representation from multi-camera images via spatiotemporal transformers, 2022c. URL <https://arxiv.org/abs/2203.17270>.

Lin, T., Dollár, P., Girshick, R. B., He, K., Hariharan, B., and Belongie, S. J. Feature pyramid networks for object detection. *CoRR*, abs/1612.03144, 2016.

Liu, W., Anguelov, D., Erhan, D., Szegedy, C., Reed, S. E., Fu, C., and Berg, A. C. SSD: single shot multibox detector. *CoRR*, abs/1512.02325, 2015.

Liu, Y., Wang, T., Zhang, X., and Sun, J. Petr: Position embedding transformation for multi-view 3d object detection, 2022a. URL <https://arxiv.org/abs/2203.05625>.

Liu, Y., Yan, J., Jia, F., Li, S., Gao, A., Wang, T., Zhang, X., and Sun, J. Petrv2: A unified framework for 3d perception from multi-camera images, 2022b. URL <https://arxiv.org/abs/2206.01256>.

Ma, Y., Wang, T., Bai, X., Yang, H., Hou, Y., Wang, Y., Qiao, Y., Yang, R., Manocha, D., and Zhu, X. Vision-centric bev perception: A survey, 2022. URL <https://arxiv.org/abs/2208.02797>.

Patil, A., Malla, S., Gang, H., and Chen, Y.-T. The h3d dataset for full-surround 3d multi-object detection and tracking in crowded urban scenes. *2019 International Conference on Robotics and Automation (ICRA)*, pp. 9552–9557, 2019.

Philion, J. and Fidler, S. Lift, splat, shoot: Encoding images from arbitrary camera rigs by implicitly unprojecting to 3d. *CoRR*, abs/2008.05711, 2020.

Redmon, J., Divvala, S. K., Girshick, R. B., and Farhadi, A. You only look once: Unified, real-time object detection. *CoRR*, abs/1506.02640, 2015.

Sun, P., Kretzschmar, H., Dotiwalla, X., Chouard, A., Patnaik, V., Tsui, P., Guo, J., Zhou, Y., Chai, Y., Caine, B., Vasudevan, V., Han, W., Ngiam, J., Zhao, H., Timofeev, A., Ettinger, S., Krivokon, M., Gao, A., Joshi, A., and Anguelov, D. Scalability in perception for autonomous driving: Waymo open dataset. In *arxiv*, pp. 2443–2451, 06 2020. doi: 10.1109/CVPR42600.2020.00252.

Tian, Z., Shen, C., Chen, H., and He, T. FCOS: fully convolutional one-stage object detection. *CoRR*, abs/1904.01355, 2019.

Vaswani, A., Shazeer, N., Parmar, N., Uszkoreit, J., Jones, L., Gomez, A. N., Kaiser, L., and Polosukhin, I. Attention is all you need. *CoRR*, abs/1706.03762, 2017.

Viola, P. and Jones, M. Rapid object detection using a boosted cascade of simple features. In *Proceedings of the 2001 IEEE Computer Society Conference on Computer Vision and Pattern Recognition. CVPR 2001*, volume 1, pp. I–I, 2001. doi: 10.1109/CVPR.2001.990517.

Wang, T., Zhu, X., Pang, J., and Lin, D. FCOS3D: fully convolutional one-stage monocular 3d object detection. *CoRR*, abs/2104.10956, 2021a.

Wang, Y., Chao, W.-L., Garg, D., Hariharan, B., Campbell, M., and Weinberger, K. Q. Pseudo-lidar from visual depth estimation: Bridging the gap in 3d object detection

for autonomous driving, 2018. URL <https://arxiv.org/abs/1812.07179>.

Wang, Y., Guizilini, V., Zhang, T., Wang, Y., Zhao, H., and Solomon, J. DETR3D: 3d object detection from multi-view images via 3d-to-2d queries. *CoRR*, abs/2110.06922, 2021b.

Xie, E., Yu, Z., Zhou, D., Phlion, J., Anandkumar, A., Fidler, S., Luo, P., and Alvarez, J. M. M²bev: Multi-camera joint 3d detection and segmentation with unified birds-eye view representation, 2022. URL <https://arxiv.org/abs/2204.05088>.

Xu, R., Xiang, H., Xia, X., Han, X., Li, J., and Ma, J. Opv2v: An open benchmark dataset and fusion pipeline for perception with vehicle-to-vehicle communication, 2021. URL <https://arxiv.org/abs/2109.07644>.

Xu, R., Tu, Z., Xiang, H., Shao, W., Zhou, B., and Ma, J. Cobevt: Cooperative bird's eye view semantic segmentation with sparse transformers, 2022. URL <https://arxiv.org/abs/2207.02202>.

Yang, C., Chen, Y., Tian, H., Tao, C., Zhu, X., Zhang, Z., Huang, G., Li, H., Qiao, Y., Lu, L., Zhou, J., and Dai, J. Bevformer v2: Adapting modern image backbones to bird's-eye-view recognition via perspective supervision, 2022. URL <https://arxiv.org/abs/2211.10439>.

Yin, T., Zhou, X., and Krähenbühl, P. Center-based 3d object detection and tracking. *CoRR*, abs/2006.11275, 2020.

Zhang, G., Luo, Z., Yu, Y., Cui, K., and Lu, S. Accelerating detr convergence via semantic-aligned matching, 2022. URL <https://arxiv.org/abs/2203.06883>.

Zhang, J., Marszalek, M., Lazebnik, S., and Schmid, C. Local features and kernels for classification of texture and object categories: A comprehensive study. *International journal of computer vision*, 73(2):213–238, 2007.

Zhu, X., Su, W., Lu, L., Li, B., Wang, X., and Dai, J. Deformable DETR: deformable transformers for end-to-end object detection. *CoRR*, abs/2010.04159, 2020.